

# Deeply Branching $c_6$ -like Cytochromes of Cyanobacteria<sup>†</sup>

Wojciech Bialek,<sup>‡</sup> Matthew Nelson,<sup>§</sup> Kamil Tamiola,<sup>‡</sup> Toivo Kallas,<sup>\*,§</sup> and Andrzej Szczepaniak<sup>\*,‡</sup>

Institute of Biochemistry and Molecular Biology, University of Wrocław, Przybyszewskiego 63/77, 51-148 Wrocław, Poland, and  
Department of Biology and Microbiology, University of Wisconsin, Oshkosh, Wisconsin 54901

Received October 1, 2007; Revised Manuscript Received January 16, 2008

**ABSTRACT:** The cyanobacterium *Synechococcus* sp. PCC 7002 carries two genes, *petJ1* and *petJ2*, for proteins related to soluble, cytochrome  $c_6$  electron transfer proteins. PetJ1 was purified from the cyanobacterium, and both cytochromes were expressed with heme incorporation in *Escherichia coli*. The expressed PetJ1 displayed spectral and biochemical properties virtually identical to those of PetJ1 from *Synechococcus*. PetJ1 is a typical cytochrome  $c_6$  but contains an unusual KDGSKSL insertion. PetJ2 isolated from *E. coli* exhibited absorbance spectra characteristic of cytochromes, although the  $\alpha$ ,  $\beta$ , and  $\gamma$  bands were red-shifted relative to those of PetJ1. Moreover, the surface electrostatic properties and redox midpoint potential of PetJ2 (pI 9.7;  $E_{m,7} = 148 \pm 1.7$  mV) differed substantially from those of PetJ1 (pI 3.8;  $E_{m,7} = 319 \pm 1.6$  mV). These data indicate that the PetJ2 cytochrome could not effectively replace PetJ1 as an electron acceptor for the cytochrome *bf* complex in photosynthesis. Phylogenetic comparisons against plant, algal, bacterial, and cyanobacterial genomes revealed two novel and widely distributed clusters of previously uncharacterized, cyanobacterial  $c_6$ -like cytochromes. PetJ2 belongs to a group that is distinct from both  $c_6$  cytochromes and the enigmatic chloroplast  $c_{6A}$  cytochromes. We tentatively designate the PetJ2 group as  $c_{6C}$  cytochromes and the other new group as  $c_{6B}$  cytochromes. Possible functions of these cytochromes are discussed.

In oxygenic photosynthesis, sunlight catalyzes electron flow from water through membrane-bound protein complexes. Mobile carriers transfer electrons between these complexes. One of these mobile carriers is cytochrome (Cyt)<sup>1</sup>  $c_6$ , a ubiquitous thylakoid lumen protein of cyanobacteria and some algal chloroplasts, which transfers electron from the cytochrome *bf* complex to the photosystem I (PS I) reaction center and, in cyanobacteria, also to a respiratory cytochrome oxidase (1, 2). Crystal structures of Cyt  $c_6$  proteins are available from several sources (3–6), and many additional sequences have been deposited in databases. These proteins are characterized by their low molecular masses (~80–90 amino acids in the mature protein), covalently bound heme, and high midpoint potentials of approximately 310–390 mV. Cyt  $c_6$  was thought to be absent from plants, having been replaced in plant and some algal electron transfer chains by the blue-copper, plastocyanin protein. More recently, a cytochrome  $c_6$ -like protein, now designated Cyt  $c_{6A}$ , has also been discovered in plants (7, 8) and the green alga *Chlamydomonas reinhardtii* (9). However, it remains

controversial whether this novel cytochrome could function as an electron carrier between the Cyt *bf* complex and PS I (8, 10–12).

All known cyanobacteria encode a Cyt  $c_6$  protein, although in some strains this can be replaced by plastocyanin under copper replete conditions (1, 13). In the cyanobacterium *Synechococcus* sp. PCC 7002, the *petJ* gene encodes Cyt  $c_6$ , which is essential for electron transfer and growth. A second gene for a putative Cyt  $c_6$  protein, designated *petJ2*, was discovered by Nomura and Bryant and its sequence deposited in the UniProt database (14) as accession number O30881. Accordingly, the original *petJ* gene was renamed *petJ1*. These authors were unable to detect the putative PetJ2 cytochrome  $c_6$  at either the protein or mRNA level in cells cultured under standard conditions. Consequently, the function of PetJ2, and indeed whether it could be expressed as a cytochrome protein, has remained obscure.

As revealed by Nomura and Bryant (15), PetJ1 of *Synechococcus* PCC 7002 is thus far unique among  $c_6$  cytochromes, because of an amino acid insertion in the mature protein (Figure 1). This insertion differs from the plant and algal Cyt  $c_{6A}$  insertion (7, 9). Moreover, and in contrast to *Synechocystis* PCC 6803 (16), the *petJ1* gene of *Synechococcus* 7002 could not be inactivated, nor could it be replaced with *petJ* (Cyt  $c_6$ ), *petE* (plastocyanin), or *cytM* (Cyt  $c_M$ ) of *Synechocystis* (15). Consequently, it appears that only the native PetJ1 cytochrome of *Synechococcus* can function properly in electron transfer and ensure cell viability.

We report here the characterization of the PetJ1 and PetJ2 cytochromes of *Synechococcus* PCC 7002. Because the PetJ2 protein has not yet been detected in *Synechococcus*, and to produce ample protein for in vitro studies, we heterologously expressed the PetJ1 and PetJ2 cytochromes

<sup>†</sup> This work was supported by NSF Grants MCB 0091415 and MCB 0450875 awarded to T.K., by NSF Grant MRI 0321545, and by the University of Wrocław Research Grants 1013/S/IBCh and N N303 3856 33 awarded to A.S.

\* To whom correspondence should be addressed. T.K.: Department of Biology and Microbiology, University of Wisconsin, Oshkosh, WI 54901; phone, (920) 424-7084; fax, (920) 424-1101; e-mail, kallas@uwosh.edu. A.S.: Institute of Biochemistry and Molecular Biology, University of Wrocław, Przybyszewskiego 63/77, 51-148 Wrocław, Poland; phone, +48 713756236; fax, +48 713756234; e-mail, andrzej.szczepaniak@ibmb.uni.wroc.pl.

<sup>‡</sup> University of Wrocław.

<sup>§</sup> University of Wisconsin.

<sup>1</sup> Abbreviations: CD, circular dichroism; Cyt, cytochrome; pI, isoelectric point; PS I, photosystem I.

in *Escherichia coli*. Both cytochromes were successfully produced with heme incorporation and exhibited spectral features typical of cytochromes, indicating that the *petJ2* gene indeed encodes a cytochrome protein. We found, however, that the electrostatic and redox properties of the PetJ1 and PetJ2 cytochromes differ radically, making it unlikely that PetJ2 could function as an electron acceptor for the Cyt *bc* complex in cyanobacterial photosynthesis. Phylogenetic analyses revealed that PetJ2 belongs to a novel and widely distributed cluster of cyanobacterial *c*-type cytochromes whose function is not yet known.

## EXPERIMENTAL PROCEDURES

**Plasmid Construction, Protein Expression, and Purification.** The *petJ1* gene was amplified from *Synechococcus* PCC 7002 DNA with primers AGCTAGCCGCGCATGGCCGCTGATGCTGCTGCTGGTGG, which introduced an *Ngo*MIV site and the last three amino acids, Ala, Met, and Ala (underlined), of the PelB transit peptide, and CTGAATTCGGATCCTTACCATTGTGTTTCTGC, which introduced a *Bam*HI site. PCR products were digested with *Ngo*MIV and *Bam*HI and inserted into plasmid pUCPF2 (17) digested with the same enzymes. The *petJ2* gene was amplified with primers GGCGATGGCCGCTGATCTCGACCAGGGAG, encoding the Ala, Met, and Ala amino acids of the PelB transit peptide, and CTGAATTCGGATCCTTAAGATTTCCAGTCGGTTTGG and inserted into pUCPF2 digested with *Nae*I and *Bam*HI. The resulting plasmids, pUCpetJ1 and pUCpetJ2, for PetJ1 and PetJ2, respectively, were confirmed by sequencing.

The *pet* genes from these plasmids were coexpressed in *E. coli* strain DH5 $\alpha$  with plasmid pEC86 (18), which carries genes for *c*-type cytochrome maturation. Fresh cotransformants were used to inoculate overnight cultures and then flasks filled to 80% capacity with LB medium. Cells were incubated at 37 °C and 220 rpm to an OD<sub>750</sub> of 0.7–1.0; the temperature was lowered to 28 °C and rpm to 80, and gene expression was induced by addition of 0.1 mM IPTG. FeSO<sub>4</sub> and  $\delta$ -aminolevulinic acid were added to concentrations of 100 and 17 mg/L, respectively. After overnight incubation, cells were harvested by centrifugation at 6000g for 10 min at 4 °C. The red cell pellets were washed in 5 mM Tris-HCl and 1 mM EDTA (pH 7.5), centrifuged, and suspended in the same buffer. Lysozyme was added to a concentration of 1 mg/mL and the suspension incubated at 37 °C for 1 h with shaking and then centrifuged at 25000g for 15 min at 4 °C. The resulting, soluble, periplasmic protein fraction was incubated with ammonium sulfate (45% saturation, 30 min, 4 °C) and centrifuged at 20000g for 20 min at 4 °C, and the pellet was discarded. Ammonium sulfate was added to the supernatant to 95% saturation and treated as described above. Supernatants containing PetJ1 or PetJ2 were dialyzed against either 20 mM Tris-HCl (pH 8) or 20 mM bis-Tris-HCl (pH 6.5) and applied to a HiTrap DEAE FF or HiTrap SP FF column (GE Healthcare), respectively. Proteins were eluted with linear 0 to 500 mM NaCl gradients. Concentrated protein fractions were further purified by size exclusion chromatography on a Superdex75 HR10/30 column. Purified proteins were characterized by SDS–PAGE and heme-staining as described in ref 19.

PetJ1 was purified from *Synechococcus* sp. PCC 7002 cells grown as described in ref 20. Cells were harvested at midlog

phase and broken by French press treatment (3  $\times$  20000 psi). PetJ1 from *Synechococcus* was purified as described above except that ammonium sulfate was added to a concentration of 70% and Q-Sepharose was used instead of DEAE FF.

**Sequence Alignments, Structure Modeling, and Phylogenetic Trees.** Sequences were aligned using ClustalX version 1.83.1: matrix BLOSUM62, gap penalty 10. Predicted structural models of the PetJ1 and PetJ2 proteins were constructed with Gromos 87 force field software (21). Parameters were as follows: SPC216 bath, 298.15 K, restrained backbone position, and 300 ps molecular dynamics runs. After 45 ps, equilibration data were collected at 10 ps steps and then averaged. Both models were deposited in the Protein Data Bank as entries 1T58 and 1T59 for PetJ1 and PetJ2, respectively. Surface electrostatic potentials were calculated with MOLMOL (22) and the Nichols and Honig algorithm (23) with parameters set to an ionic strength of 40 mM and solvent and protein dielectric constants of 80 and 4, respectively. Phylogenetic trees and bootstrap values were calculated using Neighbor Joining in PHYLIP (24).

**Circular Dichroism.** CD spectra in the ultraviolet region (UV CD) were recorded on a Jasco J-715 spectropolarimeter at 25 °C, with a 1 mm path length cell, with samples in 10 mM phosphate buffer (pH 7.0). Data points were collected every 1 nm, with six scans averaged per sample. Secondary structures were calculated from three different methods of CD spectral analysis as described previously (25).

**Mass Spectrometry and Isoelectric Focusing.** Typical parameters for electrospray ionization (ESI), ion trap mass spectrometry (Bruker Esquire 3000 Plus) were as follows: capillary voltage of 4500 V, temperature of 320 °C, drying gas at a rate of 7 L/min, and nebulizer gas pressure of 12 psi. Purified proteins were desalted on C<sub>4</sub> spin columns (Nest Group). The eluate in 50% methanol and 0.1% formic acid was injected into the mass spectrometer at a flow rate of 60–90  $\mu$ L/h. Data were analyzed with Bruker DataAnalysis. Protein isoelectric points (pI) were estimated by native isoelectric focusing (IEF) on pH 3–10 immobilized pH-gradient (IPG) strips in a Bio-Rad Protean IEF apparatus. Proteins (1  $\mu$ g) in 50 mM MOPS buffer were focused typically for 12000 Vh. pI values were calculated with QuantityOne (Bio-Rad) against Bio-Rad pI markers.

**Redox Titrations.** Redox titrations were performed as described by Dutton (26). Titrations were performed three times in both directions in a custom anaerobic cuvette, under an Ar flow, containing a platinum electrode and an Ag/AgCl<sub>2</sub> reference electrode (model MF-2052 RE-5B, Bioanalytical Systems) in 50 mM MOPS and 50 mM KCl (pH 7.0) in the presence of redox mediators: potassium ferricyanide ( $E_{m,7}$  = 430 mV), 1,1'-dimethylferrocene ( $E_{m,7}$  = 333 mV), *p*-benzoquinone ( $E_{m,7}$  = 280 mV), 1,2-naphthoquinone-4-sulfonate ( $E_{m,7}$  = 210 mV), 1,2-naphthoquinone ( $E_{m,7}$  = 145 mV), and phenazine methyl sulfate ( $E_{m,7}$  = 80 mV). Menadione (0 mV) was included for PetJ2 titrations. Potassium ferricyanide and sodium dithionite were used as the oxidant and reductant, respectively. Spectra were recorded at intervals of  $\sim$ 20 mV on an Agilent 8453 UV–visible spectrophotometer at two different mediator concentrations (20 and 50  $\mu$ M) and 1  $\mu$ M protein. Midpoint potentials were determined from the cytochrome  $\alpha$  band absorbances plotted as a function of voltage and fitted to a one-component Nernst equation with the aid of Kaleidagraph.

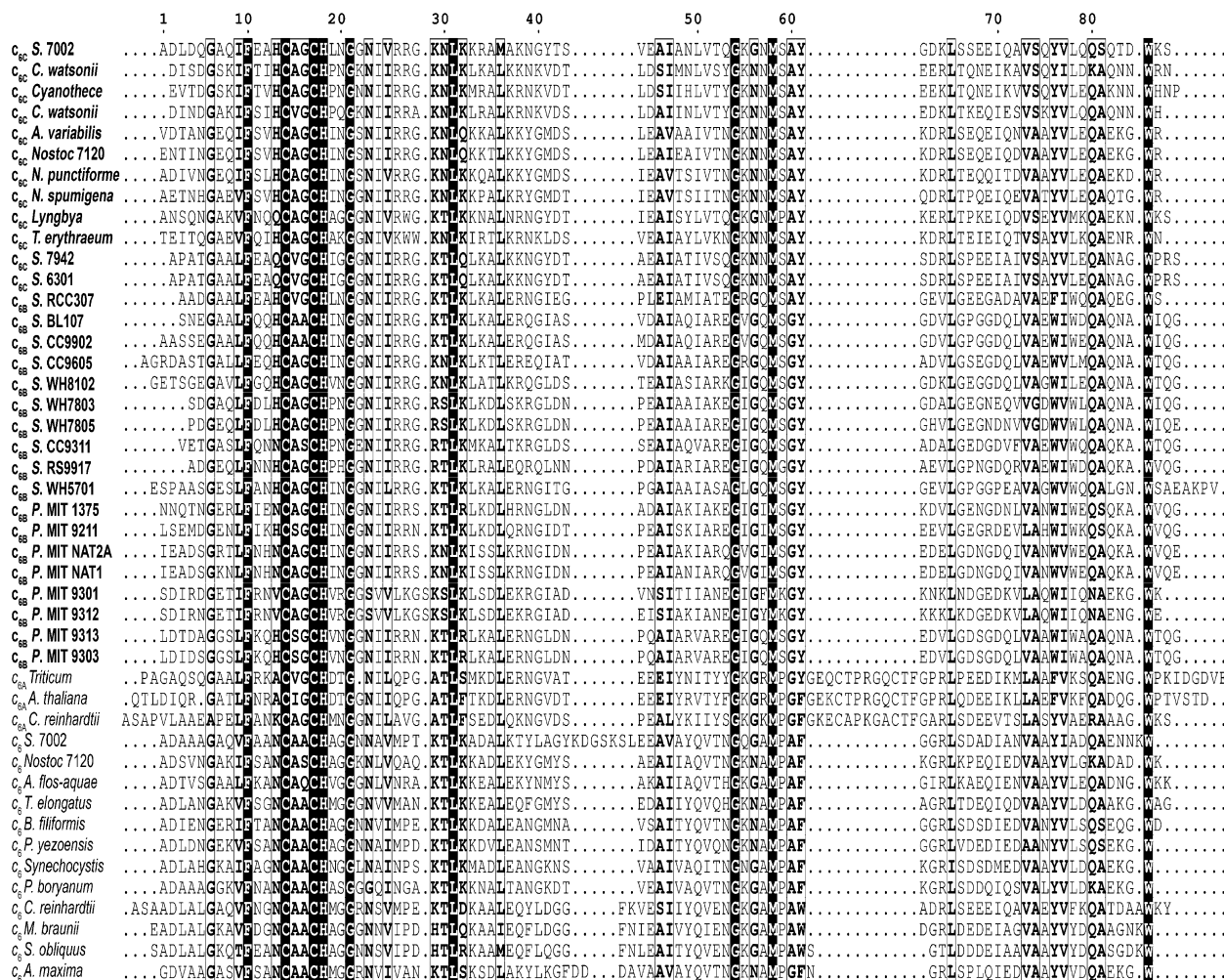


FIGURE 1: Sequence alignments of representative cyanobacterial and algal *c*<sub>6</sub> cytochromes, cyanobacterial *c*<sub>6</sub>-like cytochromes, and eukaryotic *c*<sub>6A</sub> cytochromes. Members of the two groups of *c*<sub>6</sub>-like cytochromes are listed as *c*<sub>6B</sub> or *c*<sub>6C</sub>. Residues are numbered according to the N-termini of the mature *Synechococcus* PCC 7002 PetJ1 (*c*<sub>6</sub>) and PetJ2 (*c*<sub>6C</sub>) proteins. White letters highlighted in black represent totally conserved residues, whereas similar residues are shown as black letters in boxes. The diamond (◆) at position 50 indicates a residue (Q vs I, L, or V) that may be important in determining redox properties as discussed in the text. The triangle (▲) at position 61 marks a conserved tyrosine in the *c*<sub>6</sub>-like cytochromes relative to phenylalanine or tryptophan in cytochromes *c*<sub>6A</sub> and *c*<sub>6</sub>. Sources of sequences are provided in Figure S1 of the Supporting Information.

## RESULTS

*Synechococcus* PetJ1 and PetJ2 Proteins and Other *c*-Type Cytochromes. Figure 1 displays an alignment of the *Synechococcus* sp. PCC 7002 PetJ1 and PetJ2 proteins with cyanobacterial and algal Cyt *c*<sub>6</sub> and plant and algal Cyt *c*<sub>6A</sub>. Overall, the sequences of PetJ1 and PetJ2 are 40% identical and 55% similar, on the basis of conservative amino acid substitutions. The CXXCH motif for covalent, *c*-type heme attachment is located between residues 14 and 17 of the mature PetJ1 and PetJ2 proteins. Sequence comparisons and modeling predicted that the heme axial ligands are the conserved His18 and Met65 in PetJ1 and His18 and Met58 in PetJ2. Putative signal peptides were assessed with SignalP (27), which indicated strong structural similarity in the PetJ1 and PetJ2 presequences. These consist of 117 and 115 amino acids in PetJ1 and PetJ2, respectively, including predicted 24-residue (MKKLLAIALTV-LATVFAFGTPAFA) and 28-residue (MNKRLVQVIVFVMIV-LLLVP LLATPAFG) signal peptides. This analysis suggests that the PetJ2 protein could be translocated into the thylakoid lumen, like PetJ1, or possibly the periplasmic space, which is related

in the sense of being a compartment on the “p” (positive) side of the membrane.

A striking feature of PetJ1 from *Synechococcus* sp. PCC 7002 is the KDGSKSL insertion found, thus far, exclusively in this Cyt *c*<sub>6</sub> protein. This insertion is clearly different from the 12-residue insertion found in chloroplast Cyt *c*<sub>6A</sub> proteins (Figure 1).

To better elucidate the relationship of the putative PetJ2 cytochrome to PetJ1 and other cytochromes, we performed sequence comparisons and constructed phylogenetic trees as in Figure 2. This analysis revealed discrete clusters corresponding to the expected, previously characterized *c*-type cytochromes, including *c*<sub>550</sub> associated with PS II, *c*<sub>555</sub> of *Chlorobium*, *c*<sub>6</sub> cytochromes, the chloroplast *c*<sub>6A</sub> cytochromes of unknown function, and the cryptic cyanobacterial *c*<sub>M</sub> cytochromes of unknown function (27–29). In addition, and interestingly, two new clusters appeared that branch deeply within this tree. These “*c*<sub>6</sub>-like” clusters, tentatively designated as *c*<sub>6B</sub> and *c*<sub>6C</sub>, consist entirely of previously unstudied, cyanobacterial cytochromes known only from their predicted

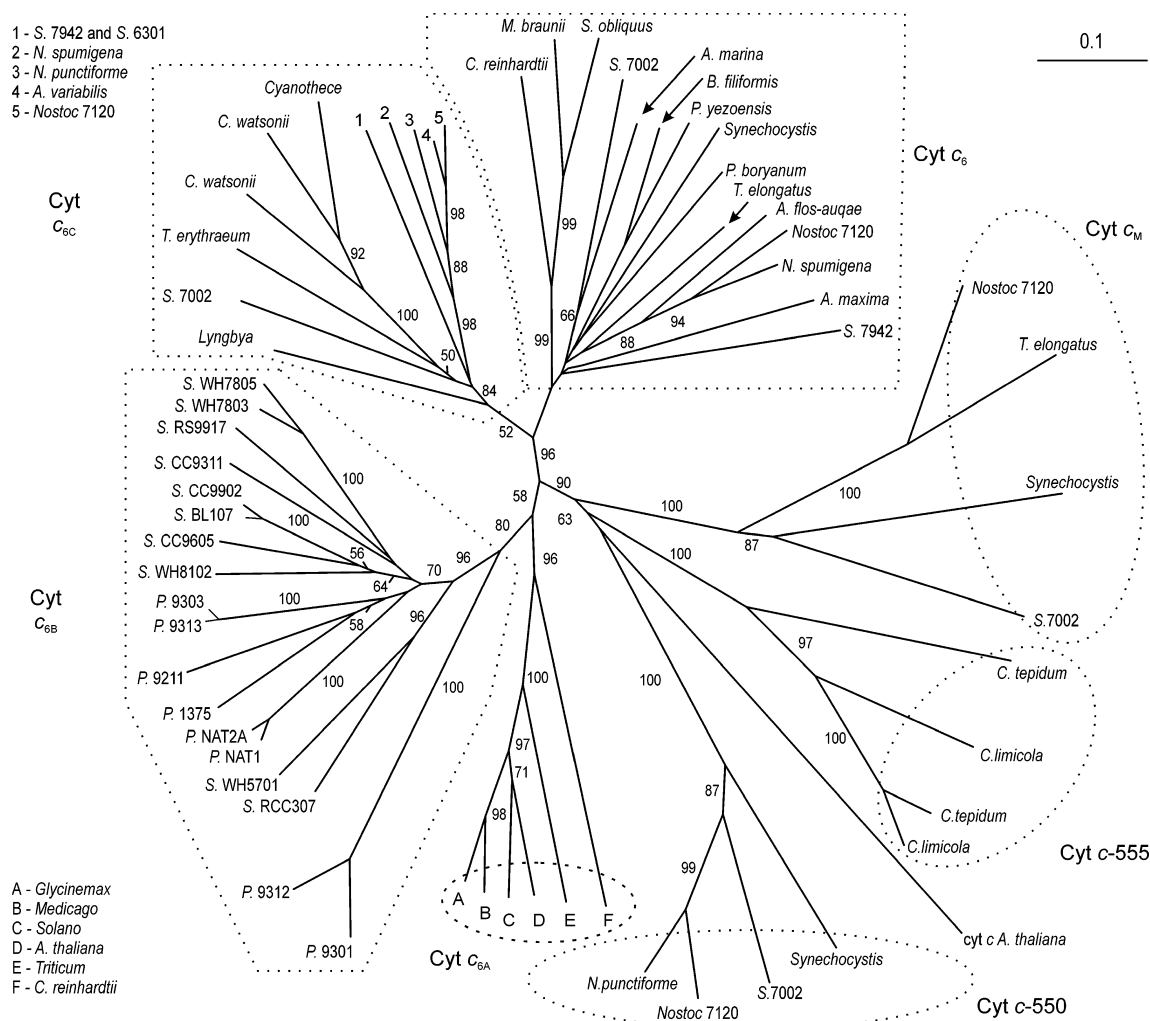


FIGURE 2: Unrooted tree of *c*-type cytochrome proteins from cyanobacteria, algae, and plants calculated using Neighbor Joining in PHYLIP (24). Bootstrap probability values of  $\geq 50$  are shown for branch points. The bar represents the approximate evolutionary distance in substitutions per residue. Sequences are from JGI and NCBI and, for *Synechococcus* sp. PCC 7002, courtesy of D. Bryant. The novel  $c_6$ -like cytochromes are encircled with a dotted line. Two clusters, labeled  $c_{6B}$  and  $c_{6C}$ , occurred consistently within this group. A comprehensive alignment and complete sequence source information are included in Figure S1 of the Supporting Information.

amino acid sequences. The cryptic *Synechococcus* PCC 7002 PetJ2 cytochrome falls within the  $c_{6C}$  group. This cluster is most closely related to the Cyt  $c_6$  group but clearly distinct from it (note the high bootstrap value of 96 at this node). The  $c_{6B}$  cytochrome cluster is more closely related to the chloroplast  $c_{6A}$  group and separated from it by a more modest bootstrap score of 58. The  $c_{6B}$  and  $c_{6C}$  clusters appear to be distinct from each other. Multiple-sequence alignment of  $c_6$ -like sequences provided further evidence that the  $c_{6B}$  and  $c_{6C}$  cytochromes comprise coherent groups (Figure 1 and Figure S1 of the Supporting Information). BLAST searches of the predicted, mature PetJ2 sequence against the  $c_{6C}$ ,  $c_{6B}$ ,  $c_{6A}$ , and  $c_6$  groups gave average amino acid sequence identities and similarities of 57.5 and 76.5%, 44.6 and 64.4%, 32.4 and 51.8%, and 43.5 and 60.1%, respectively. From these analyses, we can also conclude that the PetJ2 cytochrome is not a variant of Cyt  $c_M$  or  $c_{550}$  but rather a member of a unique,  $c_{6C}$  group of  $c_6$ -like cytochromes.

**Expression and Purification of the PetJ1 and PetJ2 Cytochromes.** To further characterize these proteins, expression plasmids were constructed and used in *E. coli*, together with plasmid pEC86 for *c*-type heme assembly (18), to overproduce the cyanobacterial cytochromes. Both PetJ1 and PetJ2 were

expressed with heme incorporation, correctly processed, and purified to homogeneity from the *E. coli* periplasm as judged by the appearance of single bands of  $\sim 9$  kDa on Coomassie-stained and TMBZ (heme)-stained SDS-PAGE gels (Figure 3A,B). These data provided the first evidence for expression of the *Synechococcus* PCC 7002 *petJ2* gene as a *bona fide* *c*-type cytochrome. Absorption spectra showing  $A_{553}/A_{274}$  or  $A_{555}/A_{274}$  ratios of 0.9 for PetJ1 and PetJ2, respectively, provided further evidence for protein purity and efficient heme incorporation (Figure 3C,D). The spectrum of PetJ1 was similar to spectra of  $c_6$  cytochromes from other species with characteristic  $\alpha$  (maximum at 553.1 nm),  $\beta$  (522.3 nm), and  $\gamma$ , or Soret (416.1 nm), bands. These data correspond well to the absorbance maxima reported by Baymann et al. (20) for the *Synechococcus* Cyt  $c_6$  in vivo. In contrast, the absorbance maxima of the PetJ2,  $c_6$ -like cytochrome were different with red-shifted  $\alpha$ ,  $\beta$ , and Soret bands in the reduced protein at 554.3, 523.2, and 417.1 nm, respectively (Figure 3C,D). The spectral features of PetJ1 expressed in *E. coli* were virtually identical to those of PetJ1 purified from *Synechococcus* (data not shown).

**Mass Spectrometry.** Correct expression and processing in *E. coli* of the PetJ1 and PetJ2 cytochromes was further verified by N-terminal sequencing of each protein (data not shown) and

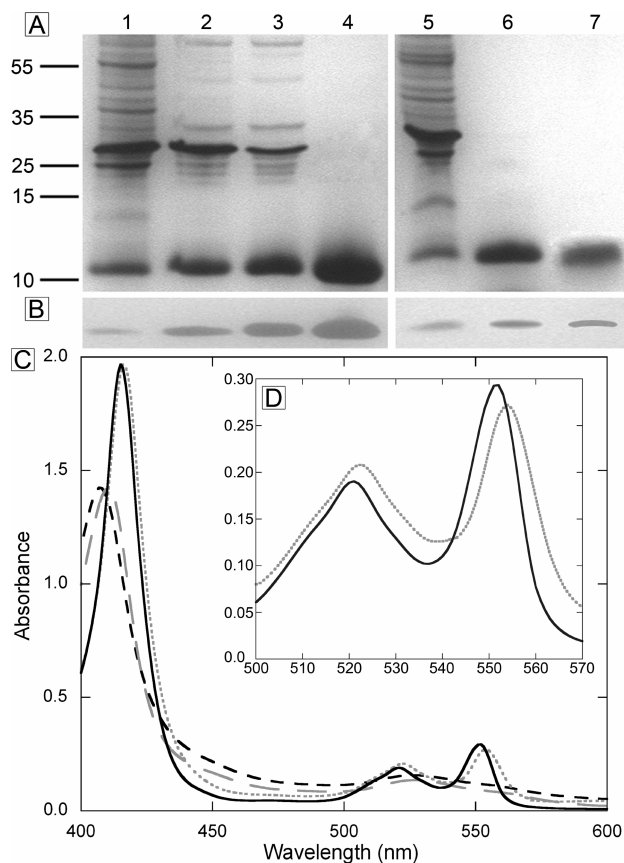


FIGURE 3: Analysis of expressed PetJ1 and PetJ2 proteins. (A) SDS-PAGE and (B) heme staining of PetJ1 (lanes 1–4) and PetJ2 (lanes 5–7) in cell lysates (lanes 1 and 5), after DEAE or Mono-Q chromatography (lanes 2 and 3), after gel filtration (lanes 4 and 7), and after SP chromatography (lane 6). (C) Normalized absorption spectra of both cytochromes: PetJ1 reduced (solid black line) and oxidized (black dashed line) and PetJ2 reduced (gray dotted line) and oxidized (gray dashed line). Cytochromes were reduced and oxidized with sodium dithionite and potassium ferricyanide, respectively. (D) Inset:  $\alpha$  and  $\beta$  peaks of PetJ1 and PetJ2.

by electrospray ionization (ESI) mass spectrometry. Figure 4 shows mass spectra of PetJ1 purified from *Synechococcus* and PetJ2 purified from *E. coli*. Electrospray ionization results in multiply charged species and therefore multiple spectral peaks that represent different charge states of the same molecule. Deconvolution of the major peaks gave a calculated average mass of 10055.2 Da for the +1 charged, intact PetJ1 protein (Figure 4B). Subtraction of the heme mass (616.48 Da) gave 9437.7 Da as the mass of the uncharged, PetJ1 apoprotein, which is within 1 Da of the mass of 9438.47 Da predicted from the sequence. Similar analyses gave the apoprotein masses of PetJ1 (not shown) and PetJ2 (Figure 4C,D) purified from *E. coli* as 9436.8 and 9400.5 Da, respectively. These values are within experimental error of the predicted masses of 9438.47 and 9400.52 Da, respectively.

**Structure Modeling and Circular Dichroism.** To gain further insight into structural features of the PetJ1 and PetJ2 cytochromes, modeling and CD analyses were performed. Modeling based on known Cyt *c*<sub>6</sub> structures generated similar, predicted three-dimensional (3D) structures for both proteins (Figure 5, top row). This overall fold is typical of Cyt *c*<sub>6</sub> proteins [e.g., the *Monoraphidium braunii* structure (Figure 5)], including Cyt *c*<sub>6A</sub>. CD spectroscopy in the ultraviolet wavelength region (UV CD) was used to gain

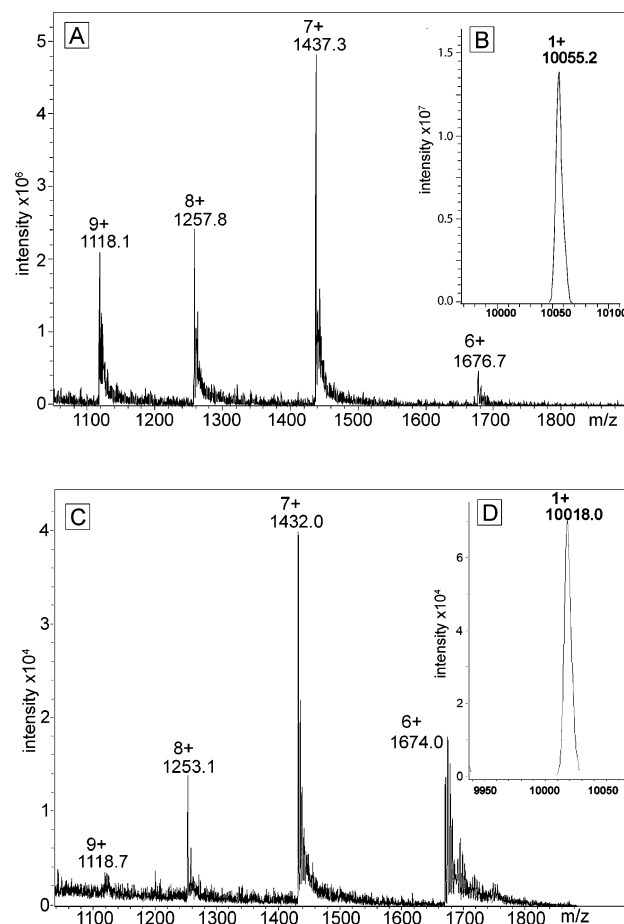


FIGURE 4: ESI mass spectra of the intact PetJ1 protein from *Synechococcus* (A) and PetJ2 protein purified from *E. coli* (C). Spectra show multiple charge states as described in the text. The insets show deconvolutions representing the predicted mass spectra and average masses of the +1 charged PetJ1 (B) and PetJ2 (D) holoproteins.

information about protein secondary structure content (28). Consistent with the overall similarity of their predicted 3D structures, the secondary structures of the PetJ1 and PetJ2 cytochromes calculated from their CD spectra were also very similar (Table 1). In contrast, the calculated surface electrostatic potential distributions of the PetJ1 and PetJ2 cytochromes differed substantially (Figure 5, bottom row).

**Isoelectric Points and Redox Midpoint Potentials.** In cyanobacteria, the electron donors to PS I may be acidic, neutral, or basic, in contrast to the acidic carriers found in eukaryotes (1, 29). In species that express both Cyt *c*<sub>6</sub> and *plastocyanin*, these proteins have similar physicochemical properties. Isoelectric focusing of the *Synechococcus* PCC 7002 PetJ1 and PetJ2 cytochromes under native conditions resulted in single, reddish bands focusing at opposite ends of the pH gradient (data not shown). The pI values determined from this analysis were 3.8 and 9.7 for the PetJ1 and PetJ2 cytochromes, respectively. These data are consistent with the very different, predominantly acidic and basic, predicted surface electrostatic potentials of these proteins (Figure 5).

Equilibrium redox titrations of the *Synechococcus* PetJ1 and PetJ2 cytochromes revealed a further, striking difference (Figure 6). Experimental data fitted to one-component Nernst equations yielded midpoint potentials ( $E_{m,7}$ ) of  $319 \pm 1.6$  mV for PetJ1 and  $148 \pm 1.7$  mV for PetJ2. The midpoint

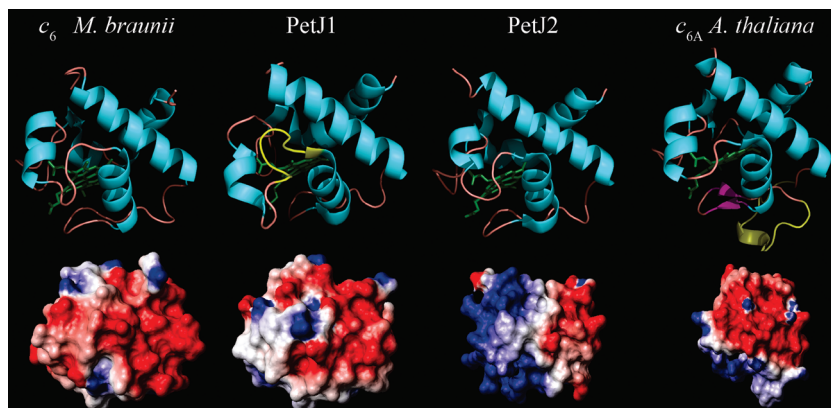


FIGURE 5: PetJ1 and PetJ2 protein structural models compared in the same orientation to the known 3D structures of Cyt  $c_6$  from *M. braunii* (3) and Cyt  $c_{6A}$  from *Arabidopsis thaliana*. Heme groups are colored green and the PetJ1 KDGSKSL and Cyt  $c_{6A}$  insertions yellow. The bottom row shows surface electrostatic potential distributions of the same cytochromes. Positively and negatively charged regions are colored blue and red, respectively.

Table 1: Secondary Structure Parameters of PetJ1 and PetJ2 Calculated from UV CD Measurements<sup>a</sup>

|           | PetJ1        | PetJ2        |
|-----------|--------------|--------------|
| helix     | 55.10 ± 6.80 | 51.75 ± 3.50 |
| strand    | 8.80 ± 2.54  | 8.50 ± 3.48  |
| turn      | 13.50 ± 4.00 | 15.83 ± 1.29 |
| unordered | 22.70 ± 5.00 | 26.82 ± 2.59 |

<sup>a</sup> The values represent the averages of means, with the standard error of the mean (SEM), of three methods of secondary structure estimation as described in Experimental Procedures.

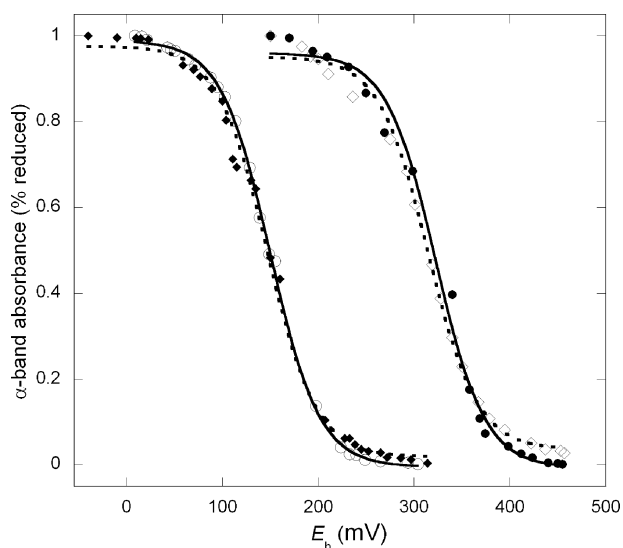


FIGURE 6: Potentiometric redox titrations of the PetJ1 (● and ◇) and PetJ2 (○ and ◆) proteins purified from *E. coli*. Titrations are shown in the oxidative (◇ and ◆) and reductive (● and ○) directions. The curves represent fits to one-electron Nernst equations which gave calculated midpoint potentials ( $E_{m,7}$ ) of  $319 \pm 1.6$  mV for PetJ1 and  $148 \pm 1.7$  mV for PetJ2.

potential of PetJ1 falls within the range of high  $E_m$  values characteristic of cyanobacterial cytochromes  $c_6$ , for example, from *Arthrosira maxima* (314 mV) or *Synechocystis* sp. PCC 6803 (320 mV) (30). In contrast, the much lower  $E_m$  of the PetJ2 protein would make this  $c_6$ -like cytochrome a very poor electron acceptor for the Cyt  $bf$  complex. The pI and redox midpoint potential of the PetJ1 Cyt  $c_6$  expressed in *E. coli* were essentially identical to those of PetJ1 isolated from *Synechococcus* sp. PCC 7002.

## DISCUSSION

**The PetJ1 Cytochrome  $c_6$  of *Synechococcus* PCC 7002.** The *Synechococcus* PetJ1 Cyt  $c_6$  contains a unique insertion loop with a possible phosphorylation motif for a CK2-type serine kinase. However, there are currently no data to demonstrate phosphorylation, and the role of this loop remains unknown. As mentioned, the enigmatic Cyt  $c_{6A}$  proteins of plant and algal chloroplasts have a highly conserved 12-residue insertion (7, 8), which is very different from the PetJ1 insertion (Figure 1). The Cyt  $c_{6A}$  insertions contain two invariant cysteines that have been postulated to serve in thiol-mediated oxidation–reduction reactions either in redox sensing (12) or in formation of disulfide bridges in thylakoid lumen proteins with concomitant electron transfer to plastocyanin (31). However, removal of the insertion loop from the *Arabidopsis*  $c_{6A}$  cytochrome altered neither its redox properties nor interaction with PS I in vitro (32). Thus, the role of the Cyt  $c_{6A}$  insertion, as well, remains unknown.

**Properties of the PetJ2  $c_6$ -like Cytochrome.** Expression of the PetJ2 protein with heme incorporation in *E. coli* confirmed that the *Synechococcus* 7002 *petJ2* gene is indeed capable of encoding a functional cytochrome. Although the overall fold of the PetJ2,  $c_6$ -like cytochrome is very similar to those of typical cytochrome  $c_6$  proteins (Figure 5) and Cyt  $c_{6A}$  (10), the physicochemical properties of the PetJ2 cytochrome differ significantly from those of the others. These properties would make the PetJ2 cytochrome a very poor electron acceptor for the Cyt  $bf$  complex [ $E_{m,7}(\text{Cyt } f) \sim 270$  mV] (20) and are consistent with the failure to inactivate PetJ1 in *Synechococcus* 7002 (15). Importantly, all  $c_6$ -like cytochromes differ from the  $c_6$  cytochromes at position 50 relative to PetJ2 (marked with a diamond in Figure 1). The  $c_6$ -like cytochromes, as well as  $c_{6A}$  cytochromes, have a small amino acid (Leu, Ile, or Val) at this position, whereas Gln occupies this site in  $c_6$  cytochromes. Interestingly, the substitution of Val for Gln ( $V > Q$ ) in Cyt  $c_{6A}$  from *A. thaliana* increased the midpoint potential by approximately 100 mV and caused a 2 nm blue shift of the  $\alpha$  band absorbance (33).

Analysis of the predicted mature amino acid sequences of representative  $c_6$ -like cytochromes revealed that most of these have basic pI values. Predicted pI values of the  $c_6$ -like cytochromes ranged from 8.05 to 9.75 for the  $c_{6C}$  group and from 4.7 to 9.0 for the  $c_{6B}$  cluster. The predicted (8.86) and

measured (9.7) pI values of PetJ2 of *Synechococcus* 7002 fall within this range. Although the midpoint potential has thus far only been determined for PetJ2 of the  $c_{6c}$  group, these observations suggest that the properties of this group of  $c_6$ -like cytochromes have been more highly conserved than those of the  $c_6$  cytochromes, where pI and surface charge can be either acidic, as in PetJ1, or basic, as in the *Anabaena/Nostoc* strains. The more distantly related *Prochlorococcus-Synechococcus*,  $c_{6B}$  cluster of  $c_6$ -like cytochromes has predicted pI values of 4.7–9.0, suggesting that these proteins may function in a different environment or serve different roles.

**Phylogeny of PetJ2 and Cyanobacterial  $c_6$ -like Cytochromes.** Data presented here reveal that the *Synechococcus* 7002 PetJ2 cytochrome belongs to a unique, previously uncharacterized, deeply branching group of cytochromes that are widely distributed throughout much of the cyanobacterial lineage. These newly discovered  $c_6$ -like cytochromes are clearly distinct from the  $c_6$  cytochromes. The  $c_{6B}$  cyanobacterial cluster is arguably not well distinguished from the chloroplast  $c_{6A}$  cytochromes on the basis of the rather low bootstrap value of 58 at the junction of these branches. However, both the  $c_{6B}$  and  $c_{6C}$ ,  $c_6$ -like cytochromes lack the 12-residue insertion that characterizes the  $c_{6A}$  proteins (Figure 1). Note also position 61 (marked by a triangle), which is occupied by a conserved tyrosine in the  $c_6$ -like sequences in contrast to phenylalanine or tryptophan in  $c_{6A}$  and  $c_6$  cytochromes. The  $c_{6C}$  cluster is comprised largely of sequences from heterocyst-forming or unicellular nitrogen-fixing cyanobacteria. PetJ2 of the unicellular cyanobacterium *Synechococcus* 7002, which does not carry *nif* genes, is an interesting exception. Recent microarray analyses provide the first evidence of transcriptional expression of members of the  $c_{6C}$  cytochrome group. The *Nostoc punctiforme* *NpF1886* gene for a  $c_6$ -like cytochrome is expressed at low but significant levels in ammonia-grown and nitrogen-starved cells and in hormogonia and akinetes (J. Meeks, University of California, Davis, CA, personal communication). The corresponding *Synechococcus* PCC 7942\_2542 gene is expressed again at low levels in control, nitrogen-starved, and sulfur-starved cells, and at a level ~2-fold lower after prolonged nitrogen depletion (R. Schwarz, Bar-Ilan University, Ramat Gan, Israel, personal communication). The  $c_{6B}$  cytochrome cluster is comprised largely of the non-nitrogen-fixing, marine *Prochlorococcus-Synechococcus* group, members of which show greater than 95% identity of 16S rRNA sequences but consist of many physiologically and genetically diverse ecotypes (34–37). In *Synechococcus* 7002, the PetJ2,  $c_6$ -like cytochrome has not yet been detected under typical laboratory culture conditions at either the mRNA or protein level. However, the widespread occurrence of  $c_6$ -like sequences among cyanobacterial lineages, and evidence of the transcription of some, suggest that these proteins are functionally expressed and confer selective advantages. Their distribution among diverse unicellular, filamentous, and nitrogen-fixing lineages suggests that they arose early in cyanobacterial evolution. Notably, however, not all cyanobacteria possess a  $c_6$ -like cytochrome. Interesting exceptions include the widely studied *Synechocystis* PCC 6803, *Gloeobacter violaceus* PCC 7421 (which lacks internal membranes), two thermophilic *Synechococcus* strains, and several strains of *Prochlorococcus marinus* (Table S1 of the Supporting Information).

**Possible Functions of PetJ2 and Cyanobacterial  $c_6$ -like Cytochromes.** Although unlikely to accept electrons from the *bf* complex, the PetJ2,  $c_6$ -like cytochrome could, at least on thermodynamic grounds, donate electrons to PS I or one of the terminal oxidases of *Synechococcus*. Some donor–PS I reactions depend on collisional interactions and can even accommodate repulsive electrostatic forces (29). Thus, electron transfer from the PetJ2  $c_6$ -like cytochrome to PS I or cytochrome oxidase cannot be ruled out *a priori* despite the seemingly unfavorable, basic surface charge of PetJ2. On the basis of its putative signal sequence, the *Synechococcus* PetJ2 could be located in the lumen, the periplasm, or both. The PetJ2 cytochrome, with a midpoint potential of ~150 mV, would be well poised to respond either to the redox potential of the quinone pool or to the environment. PetJ2 might thus interact with the CtaII heme-copper, terminal oxidase of *Synechococcus* via electron transfer and/or binding and conformation change to elicit CtaII-mediated regulation of stress responses such as those reported by Nomura and Bryant (38). Several other *c*-type cytochromes have known or postulated regulatory roles. Cyt  $c_{561}$  of *Bacillus subtilis* has a midpoint potential of ~190 mV (39) and a role in initiation of sporulation (40). Involvement of  $c_6$ -like cytochromes in redox or oxygen sensing related to heterocyst differentiation may be an intriguing possibility. Oxygen binding to the heme of the FixL sensor kinase modulates nitrogen fixation gene expression (41). Other bacterial Cyt sensors include the *Clostridium botulinum* *b*-heme SONO (42) and the *Rhodobacter capsulatus* (43) and *Alcaligenes xylosoxidans* (44) periplasmic, pentacoordinate *c'* cytochromes for sensing and/or reductive detoxification of nitric oxide (NO). Some cyanobacteria possess quinol-nitric oxide reductases as one line of defense (45).

In summary, *Synechococcus* sp. PCC 7002 PetJ2 belongs to a novel group of  $c_6$ -like cytochromes that are widely distributed among cyanobacteria and found to be transcriptionally expressed in a few strains thus far. Our analysis reveals two groups of  $c_6$ -like cytochromes that appear to have properties distinct from those of all known soluble cytochromes. We suggest that these be designated cytochromes  $c_{6B}$  and  $c_{6C}$ . These proteins may function in specific environments or serve yet-to-be-defined regulatory roles.

## ACKNOWLEDGMENT

We thank Chris Nomura and Don Bryant for the *petJ1*, *petJ2*, and subsequently *Synechococcus* sp. PCC 7002 genome sequences, William Cramer for plasmid pUCPF2, and Linda Thony-Meyer for plasmid pEC86.

## SUPPORTING INFORMATION AVAILABLE

Sequence sources for Figures 1 and 2. This material is available free of charge via the Internet at <http://pubs.acs.org>.

## REFERENCES

1. Kerfeld, C. A., and Krogmann, D. W. (1998) Photosynthetic Cytochromes *c* in Cyanobacteria, Algae, and Plants. *Annu. Rev. Plant Physiol. Plant Mol. Biol.* 49, 397–425.
2. Schmetterer, G. (1994) *Cyanobacterial Respiration*, Kluwer Academic, Dordrecht, The Netherlands.
3. Frazao, C., Soares, C. M., Carrondo, M. A., Pohl, E., Dauter, Z., Wilson, K. S., Hervas, M., Navarro, J. A., De la Rosa, M. A., and Sheldrick, G. M. (1995) Ab initio determination of the crystal

- structure of cytochrome c6 and comparison with plastocyanin. *Structure* 3, 1159–1169.
4. Kerfeld, C. A., Anwar, H. P., Interrante, R., Merchant, S., and Yeates, T. O. (1995) The structure of chloroplast cytochrome c6 at 19 Å resolution: Evidence for functional oligomerization. *J. Mol. Biol.* 250, 627–647.
  5. Sawaya, M. R., Krogmann, D. W., Serag, A., Ho, K. K., Yeates, T. O., and Kerfeld, C. A. (2001) Structures of cytochrome c-549 and cytochrome c6 from the cyanobacterium *Arthrospira maxima*. *Biochemistry* 40, 9215–9225.
  6. Yamada, S., Park, S. Y., Shimizu, H., Koshizuka, Y., Kadokura, K., Satoh, T., Suruga, K., Ogawa, M., Isogai, Y., Nishio, T., Shiro, Y., and Oku, T. (2000) Structure of cytochrome c6 from the red alga *Porphyra yezoensis* at 1.57 Å resolution. *Acta Crystallogr. D* 56, 1577–1582.
  7. Wastl, J., Bendall, D. S., and Howe, C. J. (2002) Higher plants contain a modified cytochrome c6. *Trends Plant Sci.* 7, 244–245.
  8. Gupta, R., He, Z., and Luan, S. (2002) Functional relationship of cytochrome c6 and plastocyanin in *Arabidopsis*. *Nature* 417, 567–571.
  9. Wastl, J., Purton, S., Bendall, D. S., and Howe, C. J. (2004) Two forms of cytochrome c6 in a single eukaryote. *Trends Plant Sci.* 9, 474–476.
  10. Molina-Heredia, F. P., Wastl, J., Navarro, J. A., Bendall, D. S., Hervás, M., Howe, C. J., and De La Rosa, M. A. (2003) Photosynthesis: A new function for an old cytochrome? *Nature* 424, 33–34.
  11. Weigel, M., Varotto, C., Pesaresi, P., Finazzi, G., Rappaport, F., Salamini, F., and Leister, D. (2003) Plastocyanin is indispensable for photosynthetic electron flow in *Arabidopsis thaliana*. *J. Biol. Chem.* 278, 31286–31289.
  12. Howe, C. J., Schlär-Bridley, B. G., Wastl, J., Purton, S., and Bendall, D. S. (2006) The novel cytochrome c6 of chloroplasts: A case of evolutionary bricolage? *J. Exp. Bot.* 57, 13–22.
  13. Ho, K. K., and Krogmann, D. W. (1984) Electron donors to P700 in cyanobacteria and algae: an instance of unusual genetic variability. *Biochim. Biophys. Acta* 766, 310–316.
  14. Bairoch, A., Apweiler, R., Wu, C. H., Barker, W. C., Boeckmann, B., Ferro, S., Gasteiger, E., Huang, H., Lopez, R., Magrane, M., Martin, M. J., Natale, D. A., O'Donovan, C., Redaschi, N., and Yeh, L. S. (2005) The Universal Protein Resource (UniProt). *Nucleic Acids Res.* 33, D154–D159.
  15. Nomura, C., and Bryant, D. A. (1999) Cytochrome c6 from *Synechococcus* sp. PCC 7002, in *The Phototrophic Prokaryotes* (Peschek, G., Ed.) pp 269–274, Kluwer Academic/Plenum, New York.
  16. Zhang, L., Pakrasi, H. B., and Whitmarsh, J. (1994) Photoautotrophic growth of the cyanobacterium *Synechocystis* sp. PCC 6803 in the absence of cytochrome c553 and plastocyanin. *J. Biol. Chem.* 269, 5036–5042.
  17. Ponomarev, M. V., and Cramer, W. A. (1998) Perturbation of the internal water chain in cytochrome f of oxygenic photosynthesis: Loss of the concerted reduction of cytochromes f and b6. *Biochemistry* 37, 17199–17208.
  18. Arslan, E., Schulz, H., Zufferey, R., Kunzler, P., and Thony-Meyer, L. (1998) Overproduction of the *Bradyrhizobium japonicum* c-type cytochrome subunits of the cbb3 oxidase in *Escherichia coli*. *Biochem. Biophys. Res. Commun.* 251, 744–747.
  19. Thomas, P. E., Ryan, D., and Levin, W. (1976) An improved staining procedure for the detection of the peroxidase activity of cytochrome P-450 on sodium dodecyl sulfate polyacrylamide gels. *Anal. Biochem.* 75, 168–176.
  20. Baymann, F., Rappaport, F., Joliet, P., and Kallas, T. (2001) Rapid electron transfer to photosystem I and unusual spectral features of cytochrome c6 in *Synechococcus* sp. PCC 7002 in vivo. *Biochemistry* 40, 10570–10577.
  21. Christen, M., Hunenberger, P. H., Bakowies, D., Baron, R., Burgi, R., Geerke, D. P., Heinz, T. N., Kastenholz, M. A., Krautler, V., Oostenbrink, C., Peter, C., Trzesniak, D., and van Gunsteren, W. F. (2005) The GROMOS software for biomolecular simulation: GROMOS05. *J. Comput. Chem.* 26, 1719–1751.
  22. Koradi, R., Billeter, M., and Wuthrich, K. (1996) MOLMOL: A program for display and analysis of macromolecular structures. *J. Mol. Graphics* 14, 29–32, 51–55.
  23. Nicholls, A., and Honig, B. A. (1991) *J. Comput. Chem.* 12, 435–445.
  24. Felsenstein, J. (1989) PHYLIP: Phylogeny Inference Package (Version 32). *Cladistics* 5, 164–166.
  25. Gubernator, B., Krolczewski, J., Kallas, T., and Szczepaniak, A. (2006) Iron-sulfur cluster reconstitution of spinach chloroplast Rieske protein requires a partially prefolded apoprotein. *Biochim. Biophys. Acta* 1764, 735–742.
  26. Dutton, P. L. (1978) Redox potentiometry: Determination of midpoint potentials of oxidation-reduction components of biological electron-transfer systems. *Methods Enzymol.* 54, 411–435.
  27. Bendtsen, J. D., Nielsen, H., von Heijne, G., and Brunak, S. (2004) Improved prediction of signal peptides: SignalP3. *J. Mol. Biol.* 340, 783–795.
  28. Kelly, S. M., and Price, N. C. (2000) The use of circular dichroism in the investigation of protein structure and function. *Curr. Protein Pept. Sci.* 1, 277–305.
  29. Hervás, M., Diaz-Quintana, A., Kerfeld, C. A., Krogmann, D. W., De la Rosa, M. A., and Navarro, J. A. (2005) Cyanobacterial Photosystem I lacks specificity in its interaction with cytochrome c6 electron donors. *Photosynth. Res.* 83, 329–333.
  30. Cho, Y. S., Wang, Q. J., Krogmann, D., and Whitmarsh, J. (1999) Extinction coefficients and midpoint potentials of cytochrome c6 from the cyanobacteria *Arthrospira maxima*, *Microcystis aeruginosa*, and *Synechocystis* 6803. *Biochim. Biophys. Acta* 1413, 92–97.
  31. Schlär-Bridley, B. G., Nimmo, R. H., Purton, S., Howe, C. J., and Bendall, D. S. (2006) Cytochrome c6A is a funnel for thiol oxidation in the thylakoid lumen. *FEBS Lett.* 580, 2166–2169.
  32. Wastl, J., Molina-Heredia, F. P., Hervás, M., Navarro, J. A., De la Rosa, M. A., Bendall, D. S., and Howe, C. J. (2004) Redox properties of *Arabidopsis* cytochrome c6 are independent of the loop extension specific to higher plants. *Biochim. Biophys. Acta* 1657, 115–120.
  33. Worrall, J. A., Schlär-Bridley, B. G., Reda, T., Marcaida, M. J., Moorlen, R. J., Wastl, J., Hirst, J., Bendall, D. S., Luisi, B. F., and Howe, C. J. (2007) Modulation of heme redox potential in the cytochrome c6 family. *J. Am. Chem. Soc.* 129, 9468–9475.
  34. Chisholm, S. W., Olson, R. J., Zettler, E. R., Goerick, R., Waterbury, J. B., and Welschmeyer, N. A. (1988) A novel free-living prochlorophyte abundant in the oceanic euphotic zone. *Nature* 334, 340–343.
  35. Palenik, B., and Haselkorn, R. (1992) Multiple evolutionary origins of prochlorophytes, the chlorophyll b-containing prokaryotes. *Nature* 355, 265–267.
  36. Rocap, G., Distel, D. L., Waterbury, J. B., and Chisholm, S. W. (2002) Resolution of *Prochlorococcus* and *Synechococcus* ecotypes by using 16S–23S ribosomal DNA internal transcribed spacer sequences. *Appl. Environ. Microbiol.* 68, 1180–1191.
  37. Ahlgren, N. A., and Rocap, G. (2006) Culture isolation and culture-independent clone libraries reveal new marine *Synechococcus* ecotypes with distinctive light and N physiologies. *Appl. Environ. Microbiol.* 72, 7193–7204.
  38. Nomura, C. T., Sakamoto, T., and Bryant, D. A. (2006) Roles for heme-copper oxidases in extreme high-light and oxidative stress response in the cyanobacterium *Synechococcus* sp. PCC 7002. *Arch. Microbiol.* 185, 471–479.
  39. David, P. S., Morrison, M. R., Wong, S. L., and Hill, B. C. (1999) Expression, purification, and characterization of recombinant forms of membrane-bound cytochrome c-550nm from *Bacillus subtilis*. *Protein Expression Purif.* 15, 69–76.
  40. Shin, I., Ryu, H. B., Yim, H. S., and Kang, S. O. (2005) Cytochrome c550 is related to initiation of sporulation in *Bacillus subtilis*. *J. Microbiol.* 43, 244–250.
  41. Bauer, C. E., Elsen, S., and Bird, T. H. (1999) Mechanisms for redox control of gene expression. *Annu. Rev. Microbiol.* 53, 495–523.
  42. Nioche, P., Berka, V., Vipond, J., Minton, N., Tsai, A. L., and Raman, C. S. (2004) Femtomolar sensitivity of a NO sensor from *Clostridium botulinum*. *Science* 306, 1550–1553.
  43. Cross, R., Lloyd, D., Poole, R. K., and Moir, J. W. (2001) Enzymatic removal of nitric oxide catalyzed by cytochrome c' in *Rhodobacter capsulatus*. *J. Bacteriol.* 183, 3050–3054.
  44. Kruglik, S. G., Lambry, J. C., Cianetti, S., Martin, J. L., Eady, R. R., Andrew, C. R., and Negrier, M. (2007) Molecular basis for nitric oxide dynamics and affinity with *Alcaligenes xylooxidans* cytochrome c. *J. Biol. Chem.* 282, 5053–5062.
  45. Busch, A., Friedrich, B., and Cramm, R. (2002) Characterization of the norB gene, encoding nitric oxide reductase, in the nondenitrifying cyanobacterium *Synechocystis* sp. strain PCC6803. *Appl. Environ. Microbiol.* 68, 668–672.

BI701973G